Mass transfer properties of chlorinated aromatic polyamide reverse osmosis membranes

Axel Ettori [a,b,c], Emmanuelle Gaudichet-Maurin [c], Pierre Aimar [a,b], Christel Causserand [a,b,*]

[a] Université de Toulouse, INPT, UPS, Laboratoire de Génie Chimique, 118 route de Narbonne, F-31062 Toulouse Cedex 09, France
[b] CNRS, Laboratoire de Génie Chimique, F-31062 Toulouse, France
[c] Veolia Environnement Research and Innovation, Maisons-Laffitte Research Center, Chemin de la digue – BP76, 78603 Maisons-Laffitte Cedex, France

Keywords:
Reverse osmosis
Polyamide
Chlorine
Water permeability
Swelling

A B S T R A C T

Water (*A*) and solute (*B*) permeability of aromatic polyamide (PA) reverse osmosis membranes (RO) were monitored under varying applied pressure, solute nature and concentration to assess their evolution after exposure of the membrane to free chlorine. Above a threshold value of 400 ppm h HOCl water permeability was influenced by permeation conditions during both filtration of ultrapure water (UP water) and reverse osmosis of salts performed sequentially. Water permeability decreased during the filtration of UP water performed at a constant applied pressure of 60 bar. During the reverse osmosis of an electrolyte solution, performed at a constant permeation flux of 31 L h^{-1} m^{-2}, *A* was observed to increase continuously with time, e.g. up to a factor of 3 after exposure to 3120 ppm h HOCl, most severe dose used. Differences in the charge density of mono- and divalent cations did not influence the rate of increase of *A* with time, which was however shown to depend on salt flux and ascribed to a diffusion limited relaxation process presumed to occur within the dense hydrated PA network. The relative and opposite impact of applied pressure and of salt permeation highlighted the importance in distinguishing conditions under which the water permeability (*A*) of a chlorinated membrane is measured, whether during the filtration of UP water or of a salt.

1. Introduction

Aromatic polyamide (PA) dense thin films formed by interfacial polymerization are known to possess a rigid network in part due to interchain crosslinking and to the presence of benzolyamide groups forming hydrogen bonds [1,2]. Due to this specific structural property, PA is the main component of the selective surface layer of current commercially available composite reverse osmosis (RO) membranes.

When applied to seawater desalination, the selectivity of PA based RO membranes, i.e. solute passage relative to water passage, can be altered upon exposure of these membranes to free chlorine [3], which is commonly used for oxidation of organic and inorganic compounds and for disinfection. This is due to halogen (e.g., Cl and Br) reactivity towards functional groups of the PA layer [4]. A mechanism of the chlorination of PA was proposed [5], which involves a two-step electrophilic substitution reaction, favored at acidic pH (e.g., in the presence of hypochlorous acid), which leads to both amine and aminobenzene ring chlorinated products.

Properties of chlorinated PA, either obtained by polymerization of chlorinated monomers or as is the case for RO membranes by reaction with free chlorine, have been investigated in relation to desalination performance [6,7]. Opposite results were reported in the literature regarding variations of PA interfacial properties such as hydrophilicity [8,9]. Furthermore, no measurable changes upon chlorination in surface roughness and surface charge density, as determined from streaming potential measurements, were reported in the literature, specifically under maximal manufacturer recommended exposure conditions to free chlorine (dose of 1000 ppm h) [8,10]. PA functional group chemical modifications induced by the incorporation of chlorine were observed through the entire thickness of the PA layer, as evidenced from attenuated total reflection/infrared spectra (ATR/FT-IR) [11–13], and recently from elemental analysis obtained by Rutherford backscattering spectrometry [14]. The main shifts of IR PA bands were (further) attributed to the weakening of intermolecular hydrogen bond interactions. These chemical structure modifications were proposed to alter PA chain rigidity [6,12] and mechanical properties [12,13], namely within the dense inner barrier layer defined by the PA structure model proposed by Freger and

* Corresponding author at: Université de Toulouse, INPT, UPS, Laboratoire de Génie Chimique, 118 route de Narbonne, F-31062 Toulouse Cedex 09, France. Tel.: +33 5 61 55 86 90; fax: +33 5 61 55 61 39.
E-mail address: caussera@chimie.ups-tlse.fr (C. Causserand).

Srebnik [15] and experimentally observed from elemental and free volume analysis [16,17] and microscopy images [18,19]. Of interest in the study of transport properties across PA RO membranes, chlorine-induced changes in the structure of the active layer were believed to account for the loss of filtration selectivity but also for the time dependence of water permeability observed during filtration tests performed by Kwon and Leckie [6].

In the present study, apparent transport properties, in relation to properties of chlorinated PA RO membranes described above, will be assessed specifically to address the influence of reverse osmosis operating conditions (applied pressure and solute nature and concentration) on water permeability variations reported earlier [6,12]. The intention is to clarify occasional ambiguity reported in the literature regarding water permeability variations, which will be shown to depend not only on chlorine exposure conditions but also on operating conditions in which the measurements are made. Mass transfer properties of chlorinated PA RO membranes will be further commented in relation to fractional free volume changes.

2. Materials and methods

2.1. Aqueous solutions

Filtration of single-solute aqueous solutions was performed using alternately monovalent, divalent salts or an uncharged sugar. Salts and the organic solute supplied by Acros Organics (purity of 99.5%) were stored and used as received.

Three salts with monovalent cations, NaCl, LiCl and NH_4Cl, and one with a divalent cation, $MgCl_2$ (hexahydrate), possessing the same anion (chloride ion, Cl^-) were chosen, amongst those present in seawaters, based on the relative difference of the hydration state of each cation [20]. In addition, $MgSO_4$ (heptahydrate) was chosen to vary the nature of the anion (sulfate ion SO_4^{2-}).

An uncharged organic solute, xylose (M_w = 150.3 g mol^{-1}; $\log K_{O/w} = -1.98$) [21] was also used. This hydrophilic solute is known to be retained at 90–100% by dense polyamide and polypiperazineamide based nanofiltration and reverse osmosis membranes and not to absorb to their surface [22,23].

Filtrations of NaCl solutions (the reference solute) were performed at different concentrations ranging from 0.01 M to 0.55 M NaCl. These experiments were carried out either on the same membrane sample sequentially or on separate membrane samples (done in triplicate). A constant ionic strength of 0.01 M was used during the filtration of the different salts. Filtration of xylose was performed at a concentration of 0.1 M.

Salt concentration in the retentate and in the permeate was monitored using a handheld conductivity meter (WTW, LF318). The refractive index of xylose solutions was determined using a digital refractometer (Atago RX-5000).

2.2. Membrane

A commercially available seawater reverse osmosis (RO) membrane, designated as SW30HRLE-400 (Dow FILMTEC©), was used during the entire experimental campaign. According to the manufacturer, this composite membrane is comprised of a fully aromatic polyamide (PA) thin film, the active surface layer, synthesized by interfacial polymerization on a porous polysulfone (PSf) layer supported by a polyester backing layer.

Membrane samples used for the lab-scale filtration experiments were cut on membrane sheets to a specific size with an active area of 140 cm^2. The membrane samples were extracted from an 8″ spiral-wound module and were stored between testing periods in a dark area at 4 °C in ultrapure water (UP water produced from a Millipore MilliQ system, 18.2 MΩ cm).

2.3. Characterization of membrane mass transfer properties

The transport of both water and of a solute across a RO membrane driven by a pressure difference can be described by the solution–diffusion model [24].

Water flux, J_w expressed in kg s^{-1} m^{-2} is given by the following equation:

$$J_w = \frac{P_w}{l}\cdot\frac{\rho_w\overline{V}}{RT}\cdot\Delta P = A\cdot\Delta P = A(P_{app}-\Delta\Pi) \quad (1)$$

where P_w is the intrinsic RO membrane water permeability (m^2 s^{-1}), l is the thickness of the hydrated skin (m), R is the gas constant, T the absolute temperature (K), the product of water density ρ_w and of the water molar volume $\overline{V}$ is equal to the molecular weight of pure water M_w (0.018 kg mol^{-1}), A is the RO membrane water permeability coefficient (kg s^{-1} m^{-2} Pa^{-1}) and ΔP is the net driving pressure in Pa (equal to the difference between the average feed pressure P_{app} and the trans-membrane osmotic pressure $\Delta\Pi$).

For a pure water feed solution, the trans-membrane osmotic pressure is equal to zero, thus the water flux ($J_{w,upw}$) is given by the following equation

$$J_{w,upw} = A\cdot P_{app} \quad (2)$$

In the case of the filtration of a solute, water flux ($J_{w,s}$) can be expressed by the following equation:

$$J_{w,s} = A(P_{app}-(\Pi_m-\Pi_p)) = A(P_{app}-iRT(C_m-C_p)) \quad (3)$$

In this equation the osmotic pressure is determined using the Van't Hoff equation, where C_m and C_p are the solute concentration (mol m^{-3}) at the membrane surface and in the permeate solution, respectively, and i is the number of species in solution in the case of electrolytes (it is equal to 1 for uncharged solutes).

The units more commonly used in reverse osmosis for the parameters previously defined are $J_{w,s}$ in L h^{-1} m^{-2} ($\times 2.77\times10^{-4}$ - kg s^{-1} m^{-2}), A in L h^{-1} m^{-2} bar^{-1} ($\times 2.77\times10^{-9}$ kg s^{-1} m^{-2} Pa^{-1}) and pressures P_{app} and $\Delta\Pi$ in bar. This is why these units will be used in the results and discussion sections of this paper.

Solute flux, J_s expressed in mol m^{-2} s^{-1}, can be deduced from the following equation:

$$J_s = \frac{P_s}{l}\Delta C_S = B\cdot(C_m-C_p) \quad (4)$$

where P_s is the intrinsic RO membrane solute permeability (m^2 s^{-1}), ΔC_S is the solute concentration difference and B is the RO membrane solute permeability coefficient (m s^{-1}). As for A, B depends namely on the thickness of the skin layer during permeation, l.

Using the volumetric water flux during the filtration of a solute, $J_{w,s}/\rho_w$, and the membrane rejection, R_m, given by the following equation:

$$R_m = 1-\frac{C_p}{C_m} \quad (5)$$

Eq. (6) can be derived and used to calculate B from experimentally measured quantities:

$$B = \frac{J_{w,s}}{\rho_w}\frac{1-R_m}{R_m} \quad (6)$$

To account for the concentration polarization effect during the filtration of a solute, a method described by Sutzkover et al. [25], based on the film theory and previously tested [22,26], was used to determine the osmotic pressure Π_m, and hence the solute concentration at the membrane surface (C_m) from experimentally measured quantities. This method implies that the membrane water permeability coefficient, A, should not be affected by the composition of the feed aqueous solution. In this condition, Eqs. (2) and (3) may be combined to determine Π_m:

$$\Pi_m = \Pi_p + P_{app}\left(1 - \frac{J_{w,s}}{J_{w,upw}}\right) \quad (7)$$

Water and solute permeability coefficients, corrected for the concentration polarization effects, were determined with an experimental uncertainty of 10% and 11%, respectively (resulting from instrument measurement inaccuracies).

2.4. Crossflow filtration apparatus and experimental protocol

A crossflow filtration cell (SEPA II, GE) [12] was used to perform reverse osmosis tests. A feed spacer and a permeate collector provided with the crossflow apparatus were used. UP water or a single-solute aqueous solution, contained in a 10 L stainless steel jacketed tank, was pumped to the filtration cell at a flow rate of 130 L h^{-1} (corresponding to a crossflow velocity of ca. 0.3 m s^{-1} with the equipment used). The applied pressure was controlled through adjustment of a by-pass valve and a back pressure regulator (Tescom). The permeate flux was measured volumetrically and systematically recycled back along with the retentate to the feed tank, in which the bulk feed solute concentration was kept constant. The feed solution was held at a constant temperature of 20 ± 3 °C. The pH of the aqueous solutions was 6 ± 0.5 and filtrations were performed without any adjustment.

In preparation for each experiment, the membrane samples were rinsed in UP water baths that were periodically renewed to remove preservation agents. The protocol used during the reverse osmosis filtration tests was applied similarly to membrane samples before and after chlorination. It combined three main steps which were carried out consecutively in the time span of one day:

- filtration of UP water at a constant applied pressure of 60 bar until the permeation flux $J_{w,upw}$ was constant; A was then determined;
- filtration of a solute at a permeation flux $J_{w,s}$ maintained constant at a value of 31 L h^{-1} m^{-2}; B was then calculated; and
- rinsing of the filtration apparatus and of the membrane with UP water and a final filtration of UP water at an applied pressure of 60 bar during which a final measure of A was performed.

As reported in our previous article [12], variations of the composite RO membrane water and solute permeability coefficients, discussed in Section 3, were attributed to modifications of the properties of the PA active layer.

2.5. Chlorination protocol [12]

Once the pristine membrane transport properties were measured (previous section) membranes were removed from the filtration cell and soaked, at 20 ± 3 °C, in 1 L borosilicate beakers containing free chlorine solutions prepared by diluting a 111 g L^{-1} sodium hypochlorite (NaOCl) solution in UP water to desired concentrations. The ratio of membrane area to solution volume was of 2.68 m^2 L^{-1}. The beakers were covered with Parafilm™ and stored in a dark area to reduce the natural reaction of chlorine with light or air.

The contents of hypochlorous acid (HOCl) and of the hypochlorite ion (ClO^-) were spectrophotometrically determined at three different pH units used to prepare free chlorine solutions (Agilent, HP 8452A UV–Vis spectrophotometer; HOCl: λ_{max} = 230 nm, ε_{max} = 111 M^{-1} cm^{-1}; ClO^-: λ_{max} = 292 nm, ε_{max} = 348 M^{-1} cm^{-1}). The pH was adjusted by addition of hydrochloric acid 37% v/v (Acros Organics) at values of 6.9 and 8.0, corresponding to pH conditions found in seawater desalination plants. In addition, the pH was adjusted to 5.0 where HOCl is dominant.

The contact time was set to 1 h. Chlorination of the PA RO membranes was expressed as mg h L^{-1} HOCl (ppm h HOCl). HOCl was observed to be the active specie in the chlorination of PA for a pH greater than 5.0 [12]. HOCl concentrations were converted from free chlorine concentrations using HOCl molar fractions determined spectrophotometrically at each pH. HOCl doses used during this study are presented in Table 1.

Chlorination was performed in a dark area to limit the photodegradation of pristine and chlorinated RO membrane samples [27].

3. Results

3.1. Main variations in mass transfer properties induced by chlorination

Average mass transfer properties of a set of 30 membrane samples assessed during the filtration of NaCl at a concentration of 0.55 M prior to chlorination are presented in Table 2. Variations for A, B and R_m during the filtration of 0.55 M NaCl were within the experimental uncertainties (see Section 2.3). However, it is important to point out that the measured values, corrected for the effects of concentration polarization, differed somewhat from those provided by membrane manufacturers [28]. To illustrate this point, the NaCl average retention determined during this study was equal to 97.6% in comparison to 99.8% provided by manufacturers. The measured values are nonetheless in agreement with characteristic filtration performance measurements, available in the literature, using laboratory filtration cells in comparable operating conditions (i.e. cell type, cross-flow velocity, solute concentration, and water flux) [6,17,26,29].

Fig. 1 presents the main variations of A (Fig. 1a) and B (Fig. 1b) during the filtration of UP water at 60 bar and during the subsequent filtration of 0.55 M NaCl at a constant permeation flux of 31 L h^{-1} m^{-2}. Results are given for four HOCl exposure doses (3120 ppm h, 550 ppm h, 220 ppm h, and 78 ppm h). Before chlorination (day 1), the results show a good reproducibility in membrane mass transfer properties measured for four different samples. For chlorinated membranes (day 3), in agreement with previously published results [6,12], variations of the water permeability coefficient (diamond) were observed during the filtration of UP water, marked mainly by changes in the filtration time needed for stabilization (Fig. 1a). The higher the HOCl exposure dose during the chlorination step, the faster the water flux stabilization. Fig. 1a further shows that subsequent addition of NaCl causes an immediate and continuous increase of A with time during filtration (triangle), while the permeation flux is maintained at a constant value ($J_{w,s}$ = 31 L h^{-1} m^{-2}). The increase of A was lowest for doses of 78 and 220 ppm h HOCl and more severely marked at 550 and 3120 pm h, (gray and white triangles respectively). The minimum dose at which the variations were considered to be significant was evaluated equal to 400 ppm h HOCl [12] (data not shown). Moreover, for HOCl doses higher than this value, no stabilization of A was observed in the time span of this experiment (up to 8 h). Kwon et al. did not observe a stabilization of A during the filtration of NaCl following ca. 40 h of operation in similar filtration conditions (cross-flow cell used, membrane surface area, applied pressure) for PA membranes chlorinated in similar conditions, although the rate of increase of A did decline over time [6]. The effect of the permeation of NaCl on the apparent swelling of the PA thin film was analyzed by a final measure of A with UP water (diamond in day 3). The water permeability coefficient increased by a factor of ca. 3 for series 1 by comparison with the value before salt filtration. In addition, A showed roughly no time-dependence over 1 h during the last step of the experiment. This could indicate per-

Table 1
Free chlorine doses used at pH 5.0, 6.9 and 8.0 and corresponding HOCl doses obtained using HOCl molar fractions spectrophotometrically determined for each pH.

pH	5.0	6.9			8.0		
HOCl content	~100%	78%			22%		
Free chlorine dose (ppm h)	4000	100	2500	4000	1000	2500	4000
HOCl dose (ppm h HOCl)	4000	78	1950	3120	220	550	880

Table 2
Pristine membrane mass transfer properties during the filtration of 0.55 M NaCl. Average values determined at a constant permeation flux of 31 L h^{-1} m^{-2}, 20 °C and standard deviations for 30 membranes are given.

Membrane mass transfer property	Water permeability coefficient, A (L h^{-1} m^{-2} bar^{-1})	NaCl permeability coefficient, B_{NaCl} ($\times 10^{-7}$ m s^{-1})	NaCl rejection, R_m (%)
Average value	1.35 ± 0.06	2.1 ± 0.9	97.6 ± 1.0

Table 3
Normalized NaCl permeability coefficient following chlorination at 78, 220, 550, 880, 1950, 3120 and 4000 ppm h HOCl. Average values and standard deviations obtained during tests performed in triplicate are given.

Chlorination (HOCl dose)	78 ppm h	220 ppm h	550 ppm h	880 ppm h	1950 ppm h	3120 ppm h	4000 ppm h
$B_{chlorinated}/B_{pristine}$	1.5 ± 0.1	1.4 ± 0.1	1.5 ± 0.2	2.3 ± 0.2	2.2 ± 0.3	2.5 ± 0.4	3.8 ± 0.2

manent changes of the structure of chlorinated PA with permeation of NaCl. An analogy can be made with the temperature enhanced swelling of polypiperazine nanofiltration membranes during the filtration of a salt above ambient temperature (i.e. at 50 °C), as reported by Nilsson et al. [30,31].

This experiment illustrates how the chlorinated RO membrane water permeability coefficient depends on operating conditions. Therefore water permeability coefficient values should be reported along with a full description of the operating conditions and steps (i.e., the material history).

In the absence of the stabilization of A, within the time-span during which the step of the filtration of a salt was carried out, as was the case for membranes chlorinated above 400 ppm h HOCl, the derivative of A with respect to time (A') was considered to reflect the level of RO membrane structure and performance modifications.

The profile of the solute permeability coefficient (B) with time during the filtration at a constant water flux ($J_{w,s}$ of 31 L h^{-1} m^{-2}) was marked by a sharp decrease in the earlier stages, regardless of chlorine exposure conditions and of bulk feed solute concentrations, before a stable value was reached (Fig. 1b). It the steady-state, the solute permeability coefficient was observed to increase in a stepwise fashion with increasing HOCl concentration (Table 3).

3.2. Influence of solute filtration operating conditions on water transport

3.2.1. Influence of net driving pressure

Solute filtration was performed systematically at a constant water flux to assess solute transport changes with chlorination. To balance the increase of A with time during the filtration of a solute the applied pressure was decreased so as to maintain the water flux constant (see Sections 2.4 and 3.1). This procedure corresponds to the one classically used in desalination plants where the pressure is adjusted mainly to balance the decrease of A due to fouling. On chlorinated membranes, the intention was to evaluate whether A variations during the filtration of a salt could be partly attributed to the decrease in pressure independently of the effect of salt transfer. In this objective, a control test was performed (white diamond in Fig. 2) using UP water under similar net driving pressure conditions to those used during NaCl filtration (black triangle in Fig. 2). Fig. 2 shows that before soaking in chlorine (day 1), both pristine membrane samples had similar water permeability coefficients, whether during UP water filtration (white diamond) or during NaCl filtration (black triangle). After

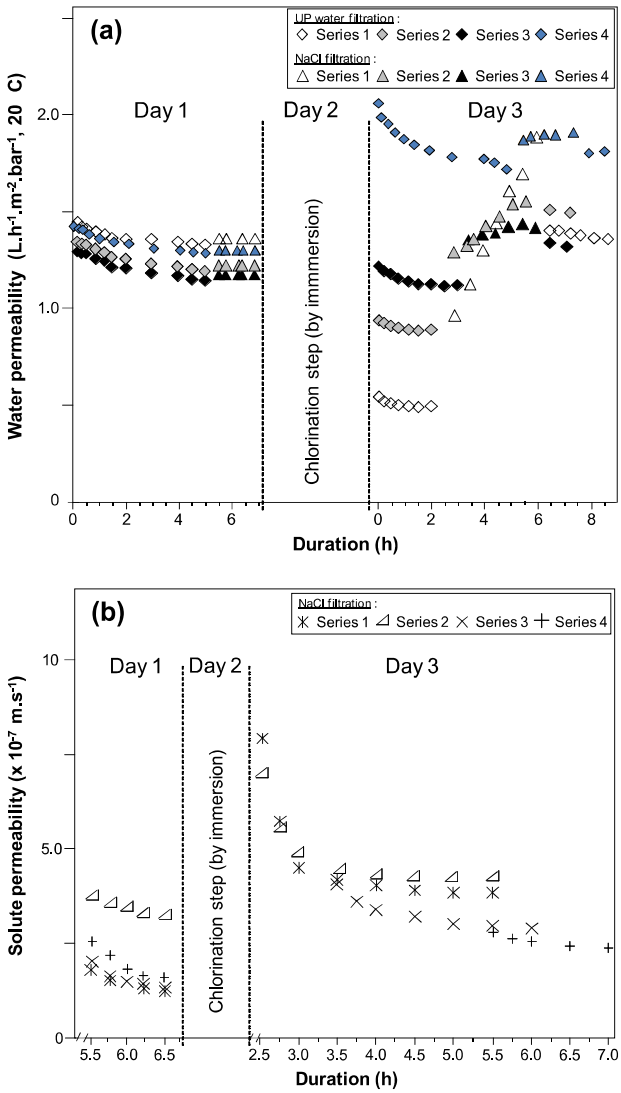

Fig. 1. (a) Water permeability coefficient (A) and (b) solute permeability coefficient (B) determined during the filtration of UP water and the subsequent filtration of NaCl at a concentration of 0.55 M before (day 1) and after (day 3) chlorination (performed on day 2). A final filtration of UP water was performed to determine the water permeability coefficient following the filtration of NaCl on day 3 (series 1: 3120 ppm h; series 2: 550 ppm h; series 3: 220 ppm h; and series 4: 78 ppm h).

chlorination (day 3) performed at 3120 ppm h HOCl, *A* decreased and stabilized at a similar value during the filtration of UP water performed at an applied feed pressure of 60 bar. When the net driving pressure was decreased, during the control test (UP water filtration), *A* increased by a factor of ca. 1.4 after 3 h (as determined during a subsequent filtration of UP water performed at 60 bar), half the increase during the filtration of NaCl (black triangle) in the same pressure conditions. Thus, a relaxation effect seems to occur upon a pressure reduction but it is much less important in the absence of salt.

3.2.2. Influence of salt flux

Repeated runs during the filtration of UP water show that variations of the water permeability coefficient due to chlorination (at a given dose) are reproducible [12]. This filtration step can be used to define an experimental starting point prior to the filtration of a salt in an attempt to apprehend, during independent tests, the influence of salt flux on the rate of increase of the water permeability coefficient with time (*A′*). It is important to stress that this approach was applied to the study of membrane samples exposed to HOCl doses above 400 ppm h, for which noticeable structure instability (i.e., decrease of *A* under applied pressure) was observed [12].

The rate of increase of *A* with time (*A′*) during the filtration of NaCl was determined at feed bulk concentrations of 0, 0.01, 0.05, 0.1 and 0.55 M during independent tests (Fig. 3a). All samples were exposed to a similar HOCl dose of 3120 ppm h, and water flux was stabilized beforehand during filtration of UP water performed at a constant feed pressure of 60 bar. The results in Fig. 3 show that *A′* (corresponding to the slope of *A* vs. time) increases with an increase in the bulk feed concentration. Furthermore, *A′* seems to level off at 0.35 L h^{-2} m^{-2} bar^{-1} for a feed bulk concentration of 0.55 M NaCl (Fig. 3-b).

Fig. 4 presents the influence of a stepwise increase in salt concentration during the filtration of NaCl carried out sequentially at concentrations of 0.05, 0.1 and 0.55 M before and after chlorination (at 3120 ppm h HOCl). In the steady-state, *B* of a pristine membrane varied by ca. 12% in the concentration range spanned. This variation is within the experimental uncertainty of *B* indicating that there seems to be no significant NaCl concentration dependence of *B* in these experimental conditions. This seems to be in agreement with AFM-thickness measurements showing the absence of swelling of the active layer of pristine RO membranes

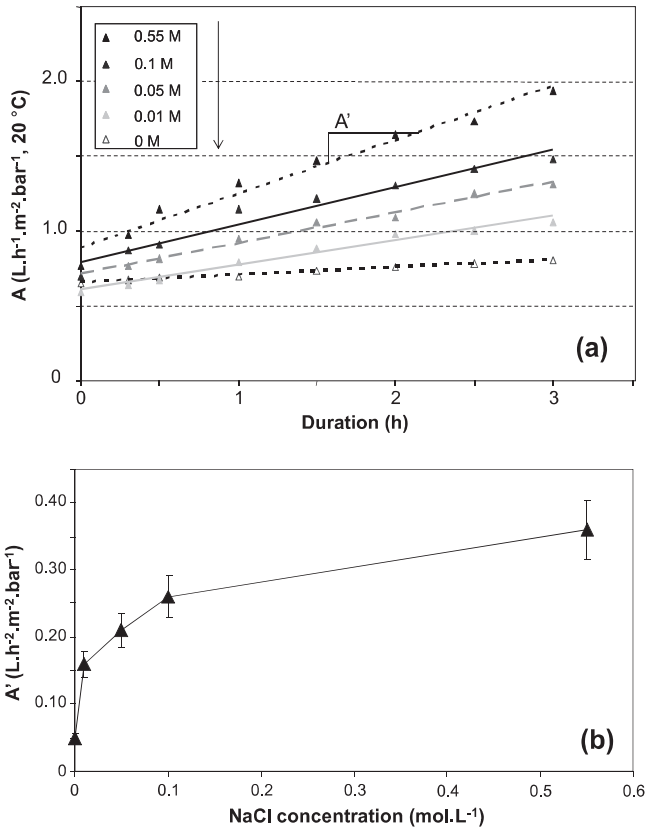

Fig. 3. (a) Usual profile of the water permeability coefficient (*A*) of chlorinated membranes versus time during the filtration of UP water and of NaCl at bulk feed concentrations of 0.01, 0.05, 0.1 and 0.55 M. The rate of increase of A with time (*A′*) corresponds to the slope of the linear regression. (b) Influence of the NaCl concentration on *A′* during the filtration performed in standard conditions ($J_{w,s}$ of 31 L h^{-1} m^{-2}, 20 °C, v_t = 0.3 m s^{-1}, pH ∼ 6.0). Membrane samples were chlorinated in similar conditions (3120 ppm h HOCl). Error bars were defined from standard deviations obtained during tests performed in triplicate.

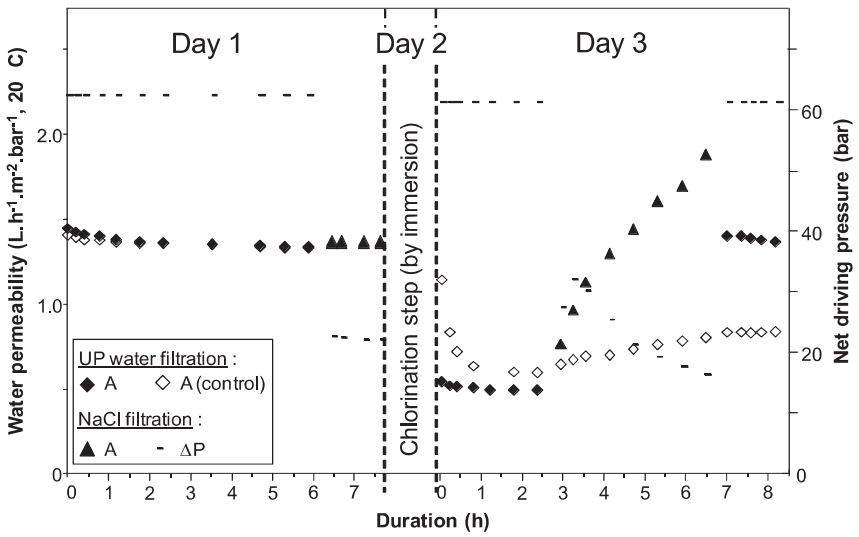

Fig. 2. Variations of chlorinated membrane water permeability coefficient (*A*) and of the net driving pressure with time. The net driving pressure was adjusted throughout the filtration of NaCl (black triangle) to maintain the permeation flux constant. The control test (white diamond) was performed to assess the influence of a decrease of the net driving pressure on the rate of increase of *A* with time during the filtration of a salt (day 3). The control test was performed with UP water during the entire procedure under similar net driving pressure conditions as those used during the filtration of 0.55 M NaCl (black triangle). Membrane samples were chlorinated in similar conditions (3120 ppm h HOCl).

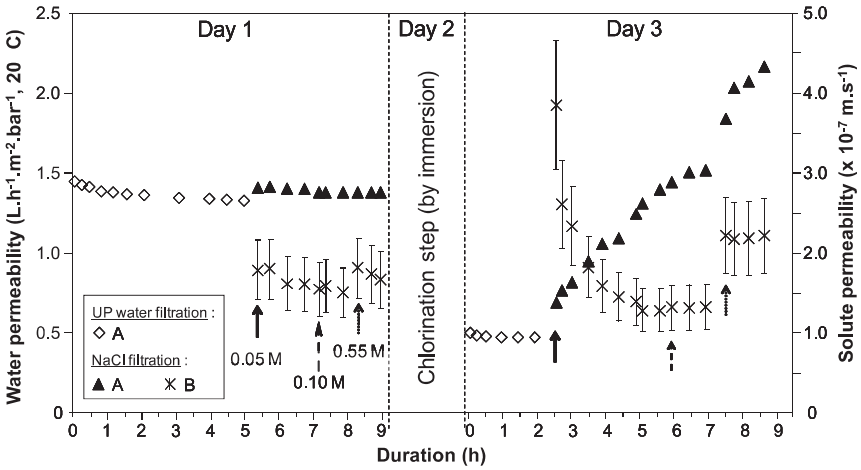

Fig. 4. Water permeability coefficient (A) and solute permeability coefficient (B) during the filtration of UP water and subsequent filtration of NaCl performed at concentrations which were increased sequentially from 0.05, 0.1 up to 0.55 M. Arrows indicate the period at which the feed aqueous solution was completed with a fresh stock solution to reach the desired NaCl concentrations. Results are given for a membrane before (day 1) and after (day 3) chlorination (performed on day 2) (3120 ppm h HOCl). Error bars correspond to the experimental uncertainty for B.

in salt solutions (in alkaline conditions) and in pure water [32]. For chlorinated membranes, an increase of the NaCl bulk feed concentration from 0.05–0.1 to 0.55 M resulted in a jump in the value of A without a noticeable change in the rate of increase (A'). At the same time, in the steady-state, B increased by ca. 70% when the bulk feed concentration was increased from 0.1 to 0.55 M.

During filtration tests performed independently on membranes exposed to 3120 ppm h HOCl, NaCl bulk feed concentration was also observed to impact on variations of B evaluated by using the normalized NaCl permeability coefficient $B_{\text{chlorinated}}/B_{\text{pristine}}$ (data not shown). In the steady state, the ratio was above 1 (the membrane had a higher permeability to NaCl after chlorination) during the filtration of an aqueous solution at a bulk feed concentration of 0.55 M NaCl, whereas it was equal to 1 during the filtration of solutions at concentrations of 0.01, 0.05 and 0.1 M NaCl. As a conclusion, the variations in the chlorinated membrane NaCl permeability coefficient exhibit the same evolution as a function of NaCl concentration whether during filtration tests performed independently at various concentrations or carried out with a sequential increase in the bulk feed concentration.

The influence of a sequential increase in the bulk feed concentration as opposed to filtration tests performed independently was also assessed in terms of variations of the water permeability coefficient. During independent filtration tests, A' increased with solute concentration (Fig. 3b). The absence of a measurable change in A' with a sequential increase in the bulk feed salt concentration (Fig. 4) seems to indicate that A is set by the initial NaCl bulk feed concentration. The same conclusions could be drawn when comparing the chlorinated membrane water permeability coefficient determined during the filtration, performed sequentially, of the different salts considered (data not shown). The results presented in Fig. 4 could arise from swelling of the hydrated PA layer during initial solute permeation, which was believed to be irreversible as determined by a measure of A during a subsequent filtration of UP water (Fig. 1a).

Fig. 5 provides an additional illustration of the impact of solute permeation, taking into account both solute concentration and nature, on changes of the PA-based RO membrane water permeability coefficient at a given chlorine exposure condition. A' is plotted against the initial solute flux (J_s, Eq. (4)) for independent filtration tests performed with salt possessing different mono- and divalent ions at a constant ionic strength of 0.01 M, with NaCl from 0.01 to 0.55 M and with xylose at a concentration of 0.1 M. Each test was performed after exposure to a HOCl dose of 3120 ppm h. It was observed that A', ascribed to structure relaxation through swelling of the PA layer, was related to the initial salt flux, irrespective of the nature of the cation for which a more detailed investigation of its influence on salt permeation through chlorinated RO membranes would be required. Essentially, salts that were most rejected, e.g. $MgSO_4$, were those that generated the lowest value of A'.

Furthermore, it seems that swelling of the PA layer was only triggered by the permeation of an electrolyte. The permeation of xylose, although enhanced after chlorination by a factor of ca. 2, did not cause any increase in A when compared to the value determined after filtration of UP water ($A' = 0$). Results on the enhanced permeation of xylose further suggest a chlorine-induced increase of segmental mobility within the PA network.

The experimental results in Fig. 5 seem to fall on a single curve (fitted and with an origin at $A'(0)$, which corresponds to the increase of A measured during the control test performed without a salt, Fig. 2) given by the following equation:

$$A' = \frac{a.J_{s,initial}}{1 + b.J_{s,initial}} \tag{8}$$

Modifications of the PA structure seem to be diffusion limited, as illustrated by the asymptote reached for A' with an increase of salt flux ($J_{s,initial}$) in these experimental conditions. In addition, the extent to which A' varies with salt flux and to which the asymptotic value is eventually reached depends on chlorine exposure conditions, i.e. the HOCl dose (white triangle in Fig. 5). A' is then proposed as an alternative probe to qualitatively assess variations of the structure of chlorinated polyamide RO membranes.

4. Discussion

Modifications of the chemistry and of the structure of aromatic polyamides caused by chlorination have yet to be fully apprehended as discussions on the exact reaction mechanism are ongoing [5,33,34]. Tang et al. 2012 recently proposed that both chlorine substitution and further covalent bond cleavage should result from exposure of PA to free chlorine. However, no reaction kinetics were provided in this study, that is there was no indication of the free chlorine doses necessary to obtain secondary bond cleavage. It has commonly been assumed that PA physicochemical property and structure changes result mainly from chlorine-induced

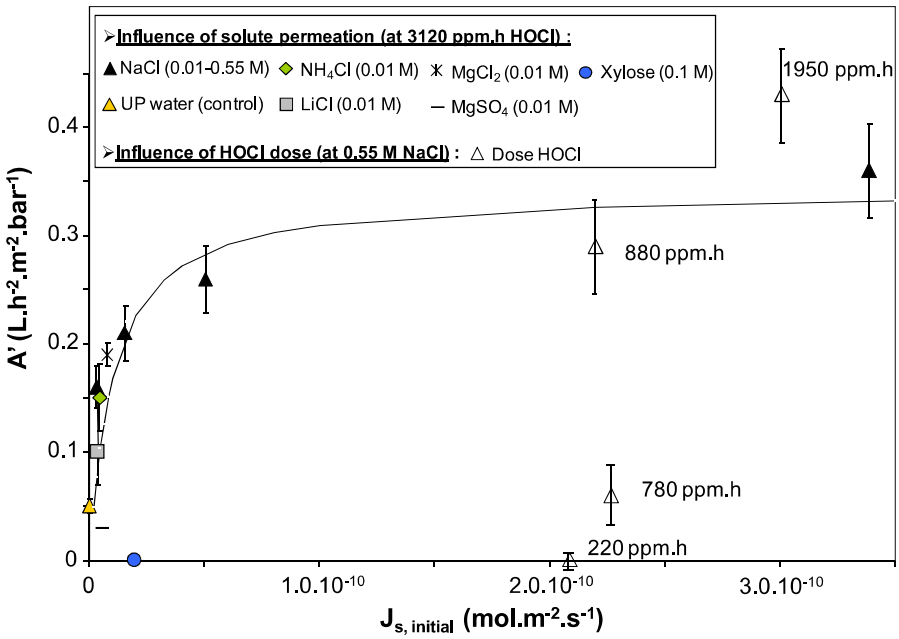

Fig. 5. Increase rate of the water permeability coefficient (A') of chlorinated membrane samples (exposed to 3120 ppm h HOCl) versus initial solute flux during the filtration of various solutes (bulk feed ionic strengths and solute concentrations are given in between parenthesis). Results on the influence of the dose of HOCl on A', determined during the filtration of NaCl with a constant bulk feed concentration of 0.55 M, are added (empty triangles). Error bars were defined from standard deviations obtained during tests performed in triplicate.

weakening of chain cohesion energy [6,9,13,35] analogously to changes observed in semi-crystalline nylon [36,37] and in amorphous PA NF membranes [38] above the glass transition.

In the present study, the pressure-induced decrease of A during the filtration of UP water, and the increase of membrane permeability to a neutral (and non-absorbing) solute such as xylose, are believed to result from a loss of rigidity within the dense PA active layer following exposure to chlorine (at doses greater than ca. 400 ppm h HOCl). The less rigid PA structure can undergo alternatively volume contraction or swelling depending on filtration conditions. As such, chlorine-induced water and solute permeability coefficient variations in relation to PA structure changes resemble temperature-enhanced relaxation of nanofiltration membranes and its impact on water and solute transport as observed the during filtration of a salt in alkaline conditions [31] and of neutral solutes [38,39].

As a consequence, a form of free volume theory can be used to describe chlorinated membrane permeability to water and to a solute, associated with PA volume contraction (polymer densification) or penetrant-induced swelling [40]. In free volume models applicable to dense polymer films, the permeation of larger hydrated solutes should show a higher dependence to free volume than that of smaller penetrants such as water [41,42].

In the experimental conditions used during this study, the hydrated PA layer of chlorinated membranes is initially believed to be in a fully densified state, following pressure-induced packing during filtration of UP water. Thus, the permeation of a hydrated ion is believed to induce swelling of the chlorinated PA layer as illustrated by the increase of A. This proposed approach could explain results reported in the literature [6] and discussed in this study on the apparent increase of the water flux, i.e. permeation flux, during the filtration of a salt at a constant net driving pressure ($\Delta\Pi$ varying on average by less than 5%), and on its time dependence as a result of polymer relaxation with the permeation of an ion. In this scheme, the increase of A as ions permeate is expected to cease once the PA network has evolved to a stable structure. Moreover, swelling within the PA layer is irreversible as shown in Fig. 1 by the increase of A as determined during the filtration of UP water performed at the end of day 3.

PA relaxation, presumed to occur during the filtration of a salt, is discussed with respect to specific filtration conditions used during this study, i.e. considering an initial filtration of UP water and its impact on PA volume contraction. However, it is believed that this process should occur, perhaps to a lesser extent, within chlorinated PA RO membranes in an actual operating environment, e.g. during seawater desalination.

The decrease and stabilization of the solute permeability coefficient, B, of chlorinated membranes during the filtration of a salt contrasts with the continuous increase of A with time. This could suggest that free volumes large enough to allow for the transport of water but too small to allow for the permeation of a hydrated ion were formed. This relatively slow process would be initiated by the penetration of ions within the less rigid chlorinated PA layer and pursued several hours after.

5. Conclusion

Filtration tests conducted at the laboratory scale have highlighted variations of RO membrane mass transfer properties when exposed, by immersion, to free chlorine, in particular to HOCl active specie in the chlorination of PA.

The sensitivity of the water permeability coefficient to pressure during the filtration of UP water, not measurable for pristine RO membranes, was associated with a decrease in rigidity within the PA active layer. Independent filtration tests of single-solute solutions, performed with different mono- and divalent salts, xylose and at different concentrations, showed that the chlorinated membrane permeability to water was influenced by the initial flux of an electrolyte ($J_{s,initial}$). These variations were enhanced with an increase in the HOCl dose. In agreement with previously published studies on the changes in PA structure and properties with

exposure to chlorine, chlorination was suggested to alter PA rigidity above an HOCl dose of 400 ppm h.

Focusing on the irreversible increase of the water permeability coefficient and its time dependence, it was shown that this phenomenon is linked to the permeation of electrolytes across the chlorinated polyamide layer. The penetration of electrolytes seems to induce a diffusion limited relaxation, through swelling, of the dense hydrated chlorinated PA layer. Three parameters, the decrease of the membrane water permeability coefficient (A) during the filtration of UP, the kinetics of the increase of the water permeability coefficient and the stabilized solute permeability coefficient (B) during the filtration of a salt, were then proposed as probes to assess chlorine-induced surface changes of RO membranes.

From an application standpoint, attention should be paid to the characterization method applied for the study of mass transfer properties of chlorinated RO membranes, specifically when the water permeability coefficient is determined, whether before or after filtration of electrolytic solutions or water.

Acknowledgement

Veolia Environnement is gratefully acknowledged for funding this work.

References

[1] J. De Abajo, J.G. De la Campa, A.E. Lozano, J.C. Alvarez, Thermally stable polymers: novel aromatic polyamides, Advanced Materials 7 (1995) 148–151.
[2] J.M. García, F.C. García, F. Serna, J.L. de la Peña, High-performance aromatic polyamides, Progress in polymer science 35 (2010) 623–686.
[3] C.J. Gabelich, J.C. Frankin, F.W. Gerringer, K.P. Ishida, I.H. Suffet, Enhanced oxidation of polyamide membranes using monochloramine and ferrous ion, Journal of Membrane Science 258 (2005) 64–70.
[4] J. Glater, M.R. Zachariah, A mechanistic study of halogen interaction with polyamide reverse-osmosis membranes, ACS Symposium Series 281 (1985) 345–358.
[5] A. Akdag, H.B. Kocer, S.D. Worley, R.M. Broughton, T.R. Webb, T.H. Bray, Why does Kevlar decompose, while Nomex does not, when treated with aqueous chlorine solutions?, Journal of Physical Chemistry B 111 (2007) 5581–5586
[6] Y.-N. Kwon, J.O. Leckie, Hypochlorite degradation of crosslinked polyamide membranes II, Changes in hydrogen bonding behavior and membrane performance, Journal of Membrane Science 282 (2006) 456–464.
[7] J. Xu, X. Feng, C. Gao, Surface modification of thin-film-composite polyamide membranes for improved reverse osmosis performance, Journal of Membrane Science 370 (2011) 116–123.
[8] Y.-N. Kwon, J.O. Leckie, Hypochlorite degradation of crosslinked polyamide membranes I. Changes in chemical/morphological properties, Journal of Membrane Science 283 (2006) 21–26.
[9] F. Serna, F. García, J.L. de la Peña, V. Calderón, J.M. García, Properties, characterization and preparation of halogenated aromatic polyamides, Journal of Polymer Research 14 (2007) 341–350.
[10] A. Simon, L.D. Nghiem, P. Le-Clech, S.J. Khan, J.E. Drewes, Effects of membrane degradation on the removal of pharmaceutically active compounds (PhACs) by NF/RO filtration processes, Journal of Membrane Science 340 (2009) 16–25.
[11] Y.-N. Kwon, C.Y. Tang, J.O. Leckie, Change of chemical composition and hydrogen bonding behavior due to chlorination of crosslinked polyamide membranes, Journal of Applied Polymer Science 108 (2008) 2061–2066.
[12] A. Ettori, E. Gaudichet-Maurin, J.C. Schrotter, P. Aimar, C. Causserand, Permeability and chemical analysis of aromatic polyamide based membranes exposed to sodium hypochlorite, Journal of Membrane Science 375 (2011) 220–230.
[13] J.Y. Chung, J.-H. Lee, K.L. Beers, C.M. Stafford, Stiffness, strength, and ductility of nanoscale thin films and membranes: a combined wrinkling–cracking methodology, Nano Letters 11 (2011) 3361–3365.
[14] O. Coronell, B.J. Mariñas, D.G. Cahill, Depth heterogeneity of fully aromatic polyamide active layers in reverse osmosis and nanofiltration membranes, Environmental Science and Technology 45 (2011) 4513–4520.
[15] V. Freger, S. Srebnik, Mathematical model of charge and density distributions in interfacial polymerization of thin films, Journal of Applied Polymer Science 88 (2003) 1162–1169.
[16] O. Coronell, B.J. Mariñas, X. Zhang, D.G. Cahill, Quantification of functional groups and modeling of their ionization behavior in the active layer of FT30 reverse osmosis membrane, Environmental Science and Technology 42 (2008) 5260–5266.
[17] S.H. Kim, S.Y. Kwak, T. Suzuki, Positron annihilation spectroscopic evidence to demonstrate the flux-enhancement mechanism in morphology-controlled thin-film-composite (TFC) membrane, Environmental Science and Technology 39 (2005) 1764–1770.
[18] V. Freger, Nanoscale heterogeneity of polyamide membranes formed by interfacial polymerization, Langmuir 19 (2003) 4791–4797.
[19] F.A. Pacheco, I. Pinnau, M. Reinhard, J.O. Leckie, Characterization of isolated polyamide thin films of RO and NF membranes using novel TEM techniques, Journal of Membrane Science 358 (2010) 51–59.
[20] B. Hribar, N.T. Southall, V. Vlachy, K.A. Dill, How ions affect the structure of water, Journal of the American Chemical Society 124 (2002) 12302–12311.
[21] L. Braeken, R. Ramaekers, Y. Zhang, G. Maes, B. van der Bruggen, C. Vandecasteele, Influence of hydrophobicity on retention in nanofiltration of aqueous solutions containing organic compounds, Journal of Membrane Science 252 (2005) 195–203.
[22] L.D. Nghiem, A.I. Schäfer, M. Elimelech, Removal of natural hormones by nanofiltration membranes: measurements, modeling, and mechanisms, Environmental Science and Technology 38 (2004) 1888–1896.
[23] L. Braeken, B. van der Bruggen, C. Vandecasteele, Flux decline in nanofiltration due to adsorption of dissolved organic compounds: model prediction of time dependency, Journal of Physical Chemistry B 110 (2006) 2957–2962.
[24] D.R. Paul, Reformulation of the solution–diffusion theory of reverse osmosis, Journal of Membrane Science 241 (2004) 371–386.
[25] I. Sutzkover, D. Hasson, R. Semiat, Simple technique for measuring the concentration polarization level in a reverse osmosis system, Desalination 131 (2000) 117–127.
[26] E.M. van Wagner, A.C. Sagle, M.M. Sharma, B.D. Freeman, Effect of crossflow testing conditions, including feed pH and continuous feed filtration, on commercial reverse osmosis membrane performance, Journal of Membrane Science 345 (2009) 97–109.
[27] H.B. Kocer, A. Akdag, S.D. Worley, O. Acevedo, R.M. Broughton, Y. Wu, Mechanism of photolytic decomposition of N-halamine antimicrobial siloxane coatings, Applied Materials and Interfaces 2 (2010) 2456–2464.
[28] G.M. Geise, H.B. Park, A.C. Sagle, B.D. Freeman, J.E. McGrath, Water permeability and water/salt selectivity tradeoff in polymers for desalination, Journal of Membrane Science 369 (2010) 130–138.
[29] E.M.V. Hoek, M. Elimelech, Cake-enhanced concentration polarization: a new fouling mechanism for salt-rejecting membranes, Environmental Science and Technology 37 (2003) 5581–5588.
[30] M. Nilsson, G. Trägårdh, K. Östergren, The influence of sodium chloride on mass transfer in a polyamide nanofiltration membrane at elevated temperatures, Journal of Membrane Science 280 (2006) 928–936.
[31] M. Nilsson, G. Trägårdh, K. Östergren, The influence of pH, salt and temperature on nanofiltration performance, Journal of Membrane Science 312 (2008) 97–106.
[32] V. Freger, Swelling and morphology of the skin layer of polyamide composite membranes: an atomic force microscopy study, Environmental Science and Technology 38 (2004) 3168–3175.
[33] J.-Y. Koo, R.J. Petersen, J.E. Cadotte, ESCA characterization of chlorine-damaged polyamide reverse osmosis membrane, ACS Polymer Preprints 27 (1986) 391–392.
[34] V.T. Do, C.Y. Tang, M. Reinhard, J.O. Leckie, Degradation of polyamide nanofiltration and reverse osmosis membranes by hypochlorite, Environmental Science and Technology 46 (2012) 852–859.
[35] S.H. Maruf, D.U. Ahn, A.R. Greenberg, Y. Ding, Glass transition behaviors of interfacially polymerized polyamide barrier layers on thin film composite membranes via nano-thermal analysis, Polymer 52 (2011) 2643–2649.
[36] C.J. Orendorff, D.L. Huber, B.C. Bunker, Effects of water and temperature on conformational order in model nylon thin films, Journal of Physical Chemistry C 113 (2009) 13723–13731.
[37] D.J. Skrovanek, S.E. Howe, P.C. Painter, M.M. Coleman, Hydrogen bonding in polymers: infrared temperature studies of an amorphous polyamide, Macromolecules 18 (1985) 1676–1683.
[38] N. Ben Amar, H. Saidani, J. Palmeri, A. Deratani, Effect of temperature on the transport of water and neutral solutes across nanofiltration membranes, Langmuir 23 (2007) 2937–2952.
[39] H. Saidani, N. Ben Amar, J. Palmeri, A. Deratani, Interplay between the transport of solutes across nanofiltration membranes and the thermal properties of the thin active layer, Langmuir 26 (2010) 2574–2583.
[40] L. Masaro, X.X. Zhu, Physical models of diffusion for polymer solutions, gels and solids, Progress in Polymer Science 24 (1999) 731–755.
[41] W. Xie, J. Cook, H.B. Park, B.D. Freeman, C.H. Lee, J.E. McGrath, Fundamental salt and water transport properties in directly copolymerized disulfonated poly(arylene ether sulfone) random copolymers, Polymer 52 (2011) 2032–2043.
[42] W. Xie, H. Ju, G.M. Geise, B.D. Freeman, J.I. Mardel, A.J. Hill, J.E. McGrath, Effect of free volume on water and salt transport properties in directly copolymerized disulfonated poly(arylene ether sulfone) random copolymers, Macromolecules 44 (2011) 4428–4438.